4760 *Chem. Mater.* **2001,** *13,* 4760−4766

# Amine-Functionalized Periodic Mesoporous Organosilicas

Mark C. Burleigh, Michael A. Markowitz,* Mark S. Spector, and Bruce P. Gaber

*Laboratory for Molecular Interfacial Interactions, Code 6930, Center for Bio/Molecular Science and Engineering, Naval Research Laboratory, Washington, D.C. 20375*

*Received June 25, 2001. Revised Manuscript Received September 25, 2001*

Ordered mesoporous materials have been synthesized by co-condensation of bis(triethoxysilyl)ethane and *N*-(2-aminoethyl)-3-aminopropyltrimethoxysilane (AAPTS) under basic conditions with supramolecular templates of cetyltrimethylammonium chloride as structure-directing agents. Incorporation of the templates into the mesoscopic composite was followed by surfactant extraction to form periodic mesoporous organosilicas. These materials have been characterized by powder X-ray diffraction, nitrogen gas sorption, metal ion adsorption, elemental analysis, and high resolution thermogravimetric analysis. The effects of AAPTS concentration in the initial solutions on the chemical and structural properties of the final products are examined.

## Introduction

Periodic mesoporous organosilicas (PMOs) are hybrid organic−inorganic materials comprising siloxane units bridged by organic groups and containing ordered mesopores.[1−6] These materials are synthesized with the surfactant template approach[7−11] whereby surfactants form supramolecular arrays in solution which become encapsulated within a solid matrix formed by condensation of the precursor. Subsequent surfactant removal results in a solid material having ordered porosity. Because these materials exhibit large internal surface areas and open pore structures, the organic bridging groups are readily accessible to molecules diffusing through the porous matrix. This is made possible by the structural rigidity imparted to these materials by the siloxane linkages. The porosity of organic polymers cannot be engineered in this way because of their inherent flexibility. Porogen removal simply results in matrix collapse, as opposed to pore formation. With both structural rigidity and organic functionality, PMOs exhibit some of the favorable properties of both organic and inorganic materials.

Although the preparation and characterization of silsesquioxane materials containing a variety of organic functional groups has been reported previously,[12−17] their syntheses did not include the use of surfactant templating. Hence, these “polysilsesquioxanes” are, in general, amorphous materials that do not contain ordered pore structures. PMOs have been synthesized by combining this known chemistry with surfactant templating. The advantages of PMOs over amorphous polysilsesquioxanes are very similar to the advantages of ordered mesoporous silica over amorphous silica. Whereas amorphous matrices contain bottlenecks that hinder molecular diffusion and accessibility to functional sites, the open pore structures of PMOs allow better accessibility and transport of molecular species. More importantly, the use of surfactant templates in the synthesis of ordered mesoporous materials allows the researcher to better control certain structural characteristics (i.e., pore size and structure, particle morphology, functional group location) by changing experimental parameters such as the choice of surfactant, reactant concentrations, and pH.

Unfortunately, not all silsesquioxane precursors can be used to create PMOs. The lack of structural rigidity in the organic portion of the silsesquioxane precursor is the limiting factor. Too much flexibility will result in a material (similar to an organic polymer) that will not hold its shape once the surfactant template is removed. For this reason, all PMOs reported to date contain

---

* Corresponding author.

(1) Inagaki, S.; Guan, S.; Fukushima, Y.; Ohsuna, T.; Terasaki, O. *J. Am. Chem. Soc.* **1999,** *121*, 9611.

(2) Melde, B. J.; Holland, B. T.; Blanford, C. F.; Stein, A. *Chem. Mater.* **1999,** *11*, 3302.

(3) Asefa, T.; MacLachlan, M. J.; Coombs, N.; Ozin, G. A. *Nature* **1999,** *402*, 867.

(4) Yoshina-Ishii, C.; Asefa, T.; Coombs, N.; MacLachlan, M. J.; Ozin, G. A. *Chem. Commun.* **1999,** 2539.

(5) MacLachlan, M. J.; Asefa, T.; Ozin, G. A. *Chem. Eur. J.* **2000,** *6*, 2507.

(6) Kruk, M.; Jaroniec, M.; Guan, S.; Inagaki, S. *J. Phys. Chem. B* **2001,** *105*, 681.

(7) Kresge, C. T.; Leonowicz, M. E.; Roth, W. J.; Vartuli, J. C.; Beck, J. S. *Nature* **1992**, *359*, 710.

(8) Beck, J. S.; Vartuli, J. C.; Roth, W. J.; Leonowicz, M. E.; Kresge, C. T.; Schmitt, K. D.; Chu, C. T.; Olsen, D. H.; Sheppard, E. W.; McCullen, S. B.; Higgens, J. B.; Schlenker, J. L. *J. Am. Chem. Soc.* **1992,** *114*, 10834.

(9) Huo, Q.; Margolese, D. I.; Stucky, G. D. *Chem. Mater.* **1996,** *8*, 1147.

(10) Tanev, P. T.; Pinnavaia, T. J. *Chem. Mater.* **1996,** *8*, 2068.

(11) Zhao, D.; Huo, Q.; Feng, J.; Chmelka, B. F.; Stucky, G. D. *J. Am. Chem. Soc.* **1998,** 120, 6024.

(12) Shea, K. J.; Loy, D. A. *Chem. Mater.* **1989,** *1*, 572.

(13) Shea, K. J.; Loy, D. A.; Webster, O. *J. Am. Chem. Soc.* **1992,** *114*, 6700.

(14) Loy, D. A.; Shea, K. J. *Chem. Rev.* **1995,** *95*, 1431.

(15) Corriu, R. J. P.; Leclercq, D. *Angew. Chem., Int. Ed. Engl.* **1996,** *35*, 1420.

(16) Cerveau, G.; Corriu, R. J. P. *Coord. Chem. Rev.* **1998,** *178−80*, 1051.

(17) Corriu, R. J. P. *Angew. Chem. Int. Ed. Engl.* **2000,** *39*, 1376.

10.1021/cm0105763 CCC: $20.00

relatively short aliphatic (ethylene, ethenylene, ethynylene) or aromatic (arylene, thiophene) moieties. Some very useful functional groups, including simple amines and thiols, have not been incorporated into PMOs, in part, because of the lack of available precursors that have the required rigidity. For instance, the organic bridging portions of known bis-trialkoxyorganosilane precursors containing amine groups {e.g., bis[3-(trimethoxysilyl)propyl]-ethylenediamine} are too flexible to “stand alone” once the porogens are extracted. Surfactant removal from the ordered mesoscopic composites of these monomers results in a collapse of the polymer matrix.[18]

We have looked at the well-documented functionalization of ordered mesoporous silicas for an alternative method to use with our PMOs. In general, functional groups have been incorporated into mesoporous silicas by either postsynthetic grafting or the co-condensation of trialkoxyorganosilanes with tetraethyl orthosilicate. The later approach, also referred to as direct synthesis, has been the preferred route for most researchers because of the easier single-pot synthetic protocol and better control of organosilane loading and distribution.[19−26] A similar approach would be to co-condense a PMO precursor with an amine-terminated trialkoxysilane to form amine-functionalized PMOs. This functionalization pathway has been used to synthesize PMOs containing the ethylenediamine moiety for metal ion sorbent applications[27] and to create PMOs containing a wide variety of functional groups.[28]

We are interested in ethylenediamine-functionalized materials with higher concentrations of functional groups and open-pore structures to enhance molecular accessibility for adsorbent and catalytic applications. However, high loading of functional organosilanes in ordered mesoporous silicas by co-condensation has been reported to diminish structural order and porosity in these materials.[26,29] Because the viability of amine-functionalized PMOs in applications involving adsorbed organic compounds or biomolecules may well depend on the loading level and porous structure of the organosilica matrix, we decided to investigate the effects of the amount of an added amine-terminated organosilane on the formation properties of the organosilica. We have prepared a series of PMOs by co-condensation of bis(triethoxysilyl)ethane (BTSE) with *N*-(2-aminoethyl)-3-aminopropyltrimethoxysilane (AAPTS) under basic conditions. Characterization of these materials has been performed with X-ray diffraction, nitrogen gas adsorption, thermogravimetric analysis, elemental analysis, and metal ion adsorption.

## Experimental Section

**Chemicals.** BTSE and AAPTS were obtained from Gelest, Inc. NaOH, HCl, cetyltrimethylammonium chloride (CTAC), and EtOH were obtained from Aldrich. All chemicals were used as received. Water used in all synthetic procedures was deionized to 18 MΩ cm.

**Synthesis.** Surfactant templates were formed under basic conditions in aqueous media, followed by the addition of BTSE and AAPTS (Figure 1). In a typical procedure, CTAC (25% w/w) was added to a polypropylene vessel containing deionized water. The solution was stirred for 5 min, followed by the addition of NaOH. Additional stirring for 10 min resulted in a clear solution. BTSE and AAPTS were mixed in a separate vial and stirred for 5 min. The silanes were then added to the surfactant solution, and the mixture was covered and stirred at room temperature for 24 h. The amount of AAPTS in the silane mixtures was varied from 5 to 30 mol %. The molar composition of the original synthetic mixtures was: 0.12 CTAC, 230 $H_2O$, 1.0 NaOH, 0.88 BTSE, 0.05−0.37 AAPTS.

**Postsynthetic Treatment.** The precipitates were recovered by suction filtration, rinsed with deionized water, and dried in vacuo at 60 °C for 6 h. A portion of these as-synthesized materials were removed for characterization of the mesoscopic composites, whereas the remainder of each sample was placed in excess (350 mL/g) acidified ethanol (1 M HCl) and refluxed for 6 h. The products were recovered by filtration, washed with ethanol, and dried under vacuum at 60 °C for 10 h. The extraction procedure was repeated twice.

**Control Samples.** A control blank in which the “silane mixture” contained only BTSE was also prepared according to the protocol described above. Another control blank, containing neither surfactant nor functional silane was also prepared. NaOH was added to deionized water under stirring, and BTSE was added. This mixture was stirred for 24 h. Hydrochloric acid was then added to adjust the pH to 8.0. The solid product was then dried under vacuum at 60 °C for 24 h. Blank material containing both BTSE and AAPTS, without any CTAC, were also synthesized by titrating to pH 8.0 with HCl.

**Characterization.** X-ray diffraction measurements were made on an Enraf-Nonius FR591 rotating-anode operating at 13 kW. A singly bent graphite monochromator selected Cu K$\alpha$ radiation and provided in-plane resolution of 0.014 $Å^{-1}$ full-width at half-maximum. Powder samples were placed in 1.0-mm quartz capillary tubes. Gas sorption experiments were performed by using a Micromeritics ASAP 2010. Nitrogen gas was used as the adsorbate at 77 K. All elemental analyses were conducted by Oneida Research Services (Whitesboro, NY). Thermogravimetric analyses were performed with a TA Instruments TGA 2950 thermogravimetric analyzer. All measurements were made in high-resolution dynamic mode under flowing nitrogen. Batch tests were performed by placing 0.050 g PMO and 10.0 mL of standardized Cu(II)/tris(hydroxymethyl)aminomethane (trizma) solutions (0.005 M) in polyethylene terephthalate (PET) vials and mixing for specific contact times. Filtrates were analyzed with a Varian 4G dual-beam UV−visible spectrometer.

## Results and Discussion

**X-ray Diffraction.** Powder X-ray diffraction analyses were performed on both the as-synthesized composites and the extracted materials. All samples exhibit a prominent peak in the diffraction pattern at approxi-

---

(18) Burleigh, M. C.; Markowitz, M. A.; Spector, M. S.; Gaber, B. P. unpublished results. Base-catalyzed polymerization of bis[3-(trimethoxysilyl)propyl]-ethylenediamine has been achieved with CTAC as the surfactant template. Nitrogen gas adsorption analyses of the surfactant-extracted product gave a calculated BET surface area of only 30 $m^2$/g. No peaks were resolved in the powder X-ray diffraction pattern.

(19) Burkett, S. L.; Sims, S. D.; Mann, S. *Chem. Commun.* **1996,** 1367.

(20) Fowler, C. E.; Burkett, S. L.; Mann, S. *Chem. Commun.* **1997,** 1769.

(21) Fowler, C. E.; Lebeau, B.; Mann, S. *Chem. Commun.* **1998,** 1825.

(22) Hall, S. R.; Fowler, C. E.; Lebeau, B.; Mann, S. *Chem. Commun.* **1999,** 201.

(23) Moller, K.; Bein, T.; Fischer, R. X. *Chem. Mater.* **1999,** *11*, 665.

(24) Lim, M. H.; Stein, A. *Chem Mater.* **1999,** *11*, 3285.

(25) Mercier, L.; Pinnavaia, T. J. *Chem. Mater.* **2000,** *12*, 188.

(26) Margolese, D.; Melero, J. A.; Christiansen, S. C.; Chemelka, B. F.; Stucky, G. D. *Chem. Mater.* **2000,** *12*, 2448.

(27) Burleigh, M. C.; Dai, S.; Hagaman, E. W. *Chem. Mater.* **2001**, *13*, 2537.

(28) Burleigh, M. C.; Markowitz, M. A.; Spector, M. S.; Gaber, B. P. *J. Phys. Chem. B* **2001**, *105*, 9935.

(29) Mercier, L.; Pinnavaia, T. J. *Chem. Mater.* 2000, *12*, 188.

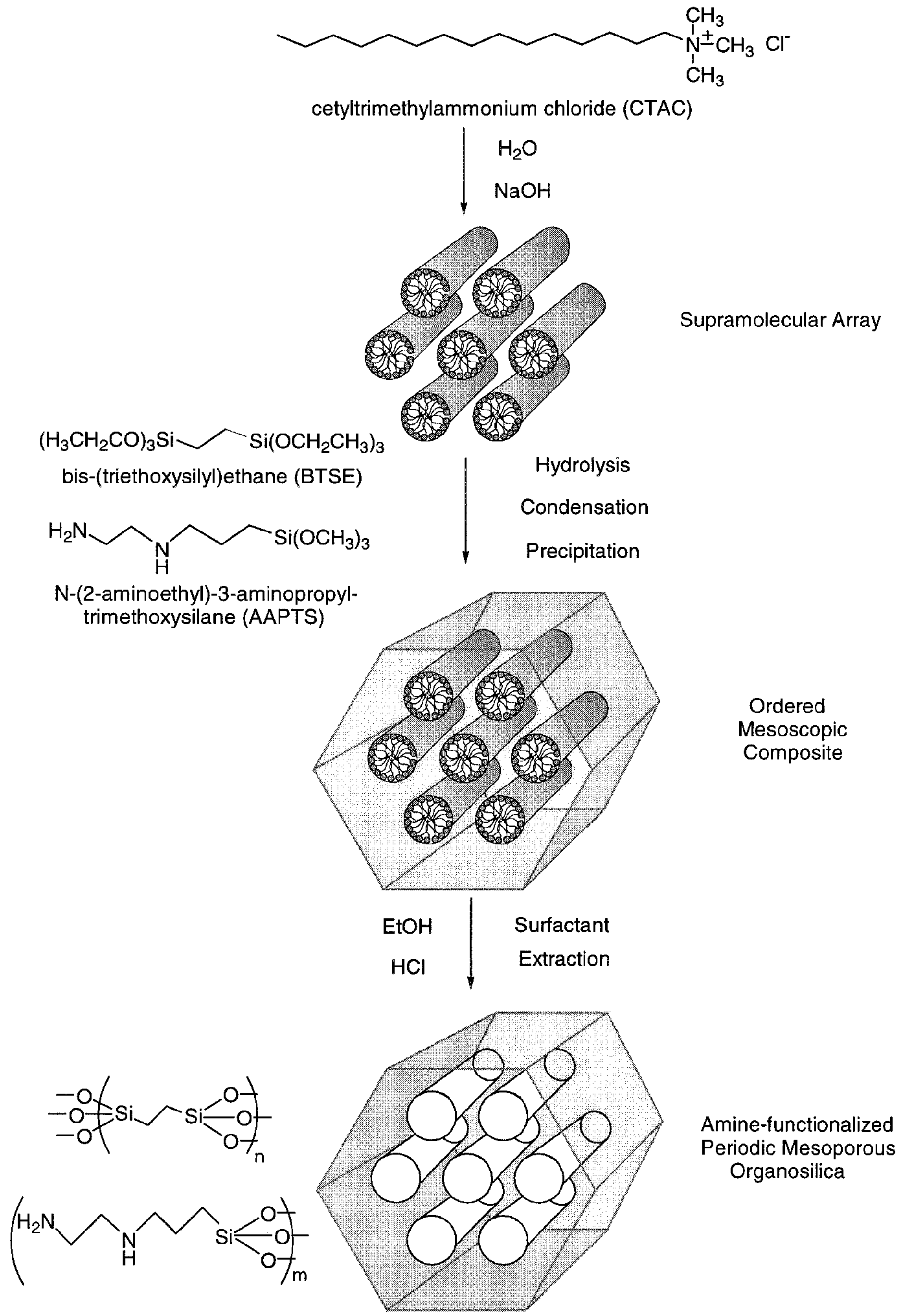

**Figure 1.** Schematic diagram of the synthesis of an amine-functionalized PMO.

**Table 1. $d_{100}$ Spacings of Organosilicas (Å)**

| sample | as-synthesized | extracted |
|---|---|---|
| control blank | 43 | 44 |
| 5 mol % AAPTS | 44 | 45 |
| 10 mol % AAPTS | 43 | 44 |
| 15 mol % AAPTS | 44 | 44 |
| 20 mol % AAPTS | 44 | 46 |
| 30 mol % AAPTS | 45 | 45 |

mately $2\theta = 2°$ characteristic of materials with long-range periodicity. This peak is usually observed for hexagonally ordered mesoporous materials. The $d_{100}$ spacings of the as-synthesized and extracted PMOs are listed in Table 1. These results indicate outstanding structural rigidity in these materials, because none of the samples exhibited any appreciable matrix contraction upon surfactant extraction. The addition of AAPTS has little effect on the $d_{100}$ spacings in these materials, indicating stable mesophase formation in basic aqueous media. No peaks were resolved in the diffraction pattern of the blank material synthesized without any surfactant, indicating that it has an amorphous structure.

**Nitrogen Sorption.** Nitrogen gas sorption analyses were performed on the extracted mesoporous samples. All the surfactant templated materials exhibit type IV isotherms and pore size distributions with maxima at approximately 26 Å. An overlay of the pore size distributions of the two control blanks is shown in Figure 2. Despite having a much larger pore volume than the nontemplated material, the templated organosilica exhibits a full width at half-maximum approximately half the size. This demonstrates the importance of surfactant templating in these materials.

**Table 2. Structural Properties of PMOs**

| sample | BET surface area (±30 $m^2/g$) | total pore volume (±0.05 $cm^3/g$) | pore diameter (±3 Å) | $a_0$[a] (±3 Å) | wall thickness[b] (±3 Å) |
|---|---|---|---|---|---|
| control blank (no surfactant) | 520 | 0.36 | | | |
| control blank | 1250 | 0.98 | 26 | 45 | 20 |
| 5 mol % AAPTS | 1020 | 0.82 | 26 | 46 | 21 |
| 10 mol % AAPTS | 1010 | 0.79 | 26 | 45 | 20 |
| 15 mol % AAPTS | 1020 | 0.79 | 26 | 45 | 20 |
| 20 mol % AAPTS | 910 | 0.74 | 26 | 47 | 22 |
| 30 mol % AAPTS | 910 | 0.67 | 25 | 46 | 22 |

[a] Calculated from $a_0 = \sqrt{[(d_{100})^2 + (r)^2]}$, where $r$ = pore radius. [b] Estimated from $a_0 - 2r$.

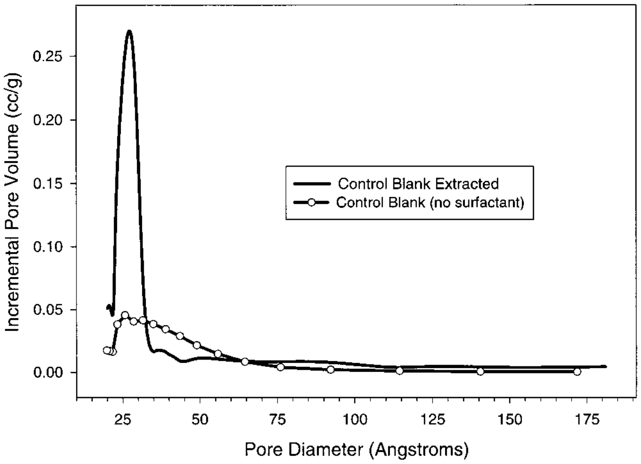

**Figure 2.** Overlay of BJH pore size distributions of the BTSE blank (no surfactant) and surfactant-templated BTSE blank materials.

The structural properties of the functionalized mesoporous organosilicas are listed in Table 2. The addition of only 5 mol % AAPTS in the original silane mixture results in a decrease in Brunauer–Emmett–Teller (BET) surface area of more than 200 $m^2/g$ relative to the templated blank sample. The further addition of AAPTS has a less pronounced effect on the final surface areas in these materials. As the concentration of AAPTS is increased, the total pore volumes decrease. Surprisingly, the concentration of AAPTS has no significant effect on the pore diameter or lattice spacing in these materials. These trends indicate that as the amount of AAPTS is increased, the size of the mesophases formed remain relatively constant, but the amount of surfactant template incorporated into these organosilicas decreases. The slight increase in the basicity of the initial reaction mixtures upon AAPTS addition may cause these changes. This would account for the decrease in both the surface areas and pore volumes, but we would then expect a marked increase in the lattice parameter.

Nitrogen sorption analyses have been performed on all the as-synthesized composites in this study. These materials exhibit surface areas of only 0.1–0.3 $m^2/g$ and no detectable pore volumes. These results are indicative of nonporous powders, impervious to dinitrogen before ethanol extraction.

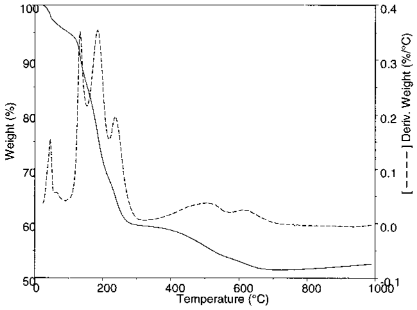

**Figure 3.** Thermogravimetric weight-loss curve and derivative plot of as-synthesized BTSE blank composite organosilica.

**Thermogravimetric Analysis.** Thermogravimetric analyses of the as-synthesized composites (Figure 3) and extracted organosilicas (Figure 4) were conducted from room temperature to 1000 °C. The weight-loss curves of the as-synthesized materials are dominated by the relatively large loss (30–35 wt %) caused by the decomposition of the alkylammonium surfactant. This loss is characterized by three overlapping peaks in the plot of the derivative of the weight-loss curve. A loss of approximately 5 wt % at temperatures below 120 °C, because of the loss of residual ethanol and water, is followed by surfactant decomposition from 120 to 300 °C. Gradual matrix decomposition from 300 to 700 °C accounts for an additional loss of 8–10 wt %. Matrix decomposition gives two relatively broad peaks in the derivative plot. Any loss due to the decomposition of grafted AAPTS is not seen because it occurs in the same temperature range as that of the surfactant.

The weight-loss curves and corresponding derivative plots of the extracted organosilicas (Figure 4a–f) show no evidence of any residual surfactant. Several trends are apparent as the AAPTS concentration is increased from zero (control blank, Figure 4a) to 30 mol % (Figure 4f). The amount of adsorbed ethanol increases from less than 2 wt % to about 5 wt %. This indicates the increase in surface hydrophilicity caused by the increase in concentration of amine groups. The weight loss caused by decomposition of the grafted AAPTS from 120 to 300 °C increases significantly, but it is hard to quantify because it overlaps with the matrix weight loss. Even though the AAPTS weight loss occurs in the same temperature range as that of the surfactant, it has a different shape. Unlike the three peaks found in the derivative plot of the surfactant weight loss, AAPTS gives only a single peak. The loss due to AAPTS is also more gradual, not reaching its fastest rate until about 280 °C.

The extracted control blank sample exhibits a significant weight gain at temperatures above 700 °C. This increase may be caused by the formation of oxides or nitrides from reactions between the purge gas and the decomposition products. Even though this range of temperatures is not of particular interest to us, such a weight gain is surprising nonetheless. The as-synthesized composites did not exhibit such a weight gain. Furthermore, the extracted samples containing the most AAPTS exhibit the smallest weight gains above 700 °C. These results suggest that carbonaceous residues from

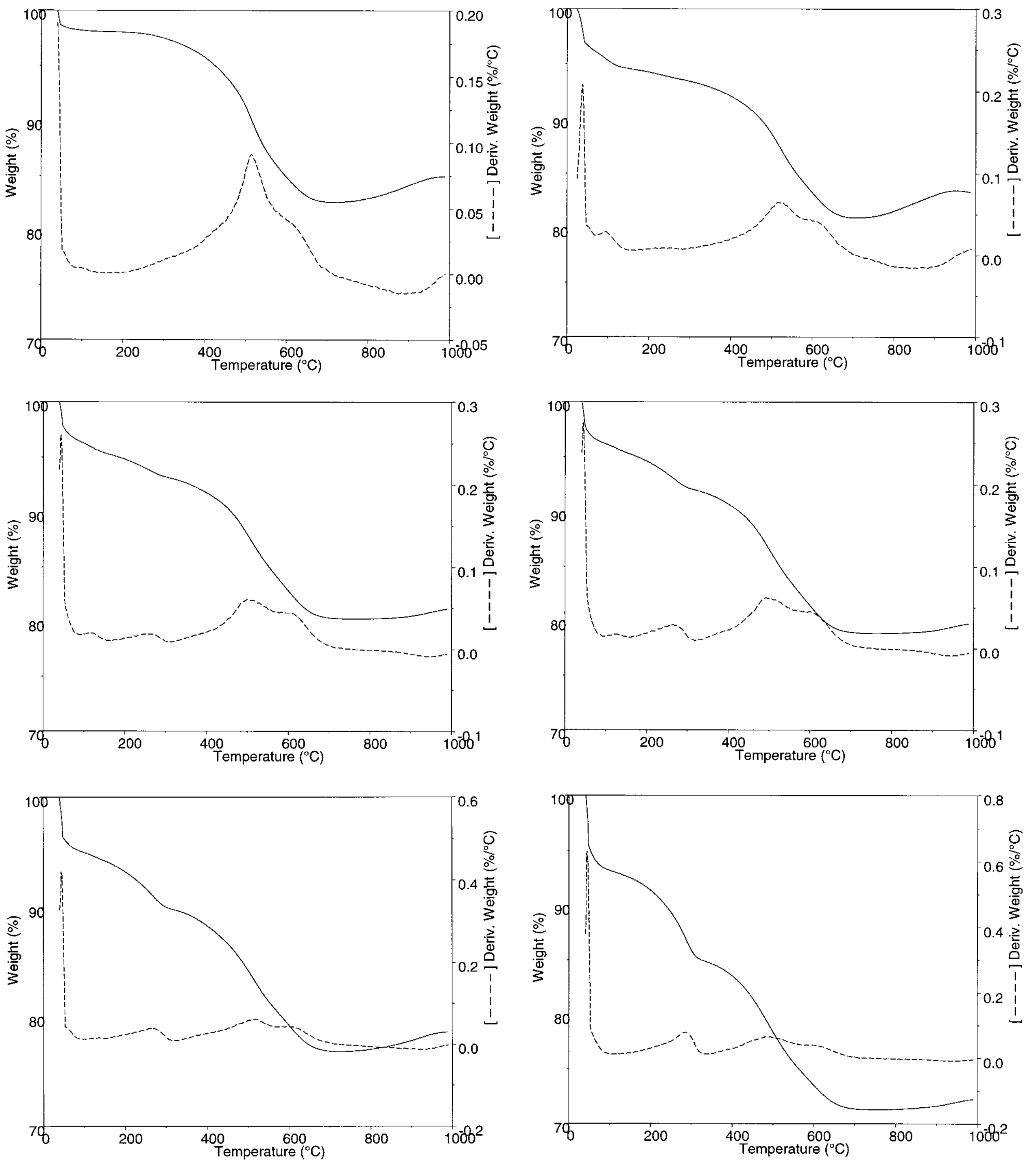

**Figure 4.** Thermogravimetric weight-loss curves and derivative plots of extracted (a) BTSE blank, (b) 5 mol % AAPTS, (c) 10 mol % AAPTS, (d) 15 mol % AAPTS, (e) 20 mol % AAPTS, and (f) 30 mol % AAPTS PMOs.

both the surfactant and grafted AAPTS decrease matrix reactivity with oxygen and/or nitrogen from the purge stream. This would effectively reduce the overall weight gain at these higher temperatures.

**Elemental Analysis.** Elemental analyses of the extracted organosilicas were used for quantitative determinations of AAPTS in the final products. Mole percentages of AAPTS in the initial reaction mixtures and resulting organosilicas are listed in Table 3. A comparison shows that only about one third of the AAPTS in the original mixtures is incorporated into the organosilica products, most likely because of the faster condensation rate of AAPTS.[28] If the faster reacting AAPTS molecules undergo homocondensation instead of condensing with BTSE, then they are unable to form the siloxane linkages necessary to incorporate them into

**Table 3. Incorporation of AAPTS in Organosilicas**

| sample (initial mol %) | extracted product[a] |
|---|---|
| AAPTS 5 mol % | 1.8 |
| AAPTS 10 mol % | 3.2 |
| AAPTS 15 mol % | 4.4 |
| AAPTS 20 mol % | 6.1 |
| AAPTS 30 mol % | 9.4 |

[a] Mole percentages estimated by elemental analysis (±1.5 mol %).

**Table 4. Accessibility of AAPTS Sites in Organosilicas**

| sample (initial mol %) | bulk AAPTS[a] (mmol/g) | accessible AAPTS[b] (mmol/g) | percentage accessible AAPTS |
|---|---|---|---|
| AAPTS 5 mol % | 0.17 | 0.14 | 82.4 |
| AAPTS 10 mol % | 0.31 | 0.25 | 80.6 |
| AAPTS 20 mol % | 0.57 | 0.44 | 77.2 |
| AAPTS 30 mol % | 0.87 | 0.61 | 70.1 |

[a] Estimated by elemental analysis. [b] Estimated by copper(II) adsorption.

the matrix. The resulting clusters would be washed out of the composite material during the extraction step.

**Metal Ion Adsorption.** Although elemental analysis by combustion can be used to estimate the concentration of the functional silane in the bulk material, it does not give information on the location of the functional sites within a sample. To make efficient sorbent, sensor, or catalytic materials, the functional sites need to be readily accessible for further reactions. We have estimated the accessibility of the diamine functional groups by the adsorption of Cu(II)/trizma complexes from aqueous solutions (pH 7.5). The trizma serves two functions in this system. First, it forms a pH buffer with a p$K_a$ of 8.1. Second, it forms strongly colored complexes with the Cu(II) ion ($\lambda_{max}$ = 640 nm) that can used as a probe to monitor the adsorption of Cu(II) to the organosilica. A large excess of trizma (0.1 M) with respect to copper (0.005 M) ensures both buffer capacity and coordinative saturation of the cupric ion. In general, chelating diamine moieties form much more stable complexes with copper(II) than ligands such as trizma that contain only a single amine. Therefore, our diamine-functionalized organosilica should readily adsorb Cu(II) from the trizma-containing solution. The removal of the Cu(II) from the solutions was measured by UV/visible spectroscopy.

The change in Cu(II) concentration of the buffered solutions during batch tests (1-h contact time) was used to calculate the number of copper(II) ions adsorbed by our organosilicas. This has been used as an indirect measurement of the number of accessible diamine functionalities in these materials by assuming 1:1 Cu(II)/diamine complex formation. A 1:1 complex is formed, because a large excess of Cu(II) is present and $K_1 > K_2$ for Cu(II)/diamine complexes.[30] A comparison of the AAPTS in the extracted PMOs measured by elemental analysis to the AAPTS accessible to Cu(II) ions is given in Table 4. As the amount of functional silane increases, the percentage of accessible sites decreases from ~80 to 70. This loss is more than offset by the overall increase in functional groups, and higher diamine content therefore always corresponds to a greater number of accessible functional sites per gram.

Batch tests were also performed on three different control blank samples. Control samples synthesized without AAPTS (with and without CTAC) did not adsorb any detectable amount of Cu(II). A third control, synthesized with BTSE and AAPTS (30 mol %), but without CTAC, adsorbed only 0.05 mmol Cu(II)/g. This represents less than 10% of the amount (0.61 mmol Cu(II)/g) adsorbed by the corresponding PMO synthesized with the surfactant. The utility of the surfactant in the synthesis of these materials is demonstrated not only by this marked increase in functional accessibilty, but also in the overall reactivity of the precursor solutions. Although all synthetic mixtures containing CTAC readily formed product via precipitation, those without CTAC did not. For example, attempts were made to prepare control samples with no CTAC, BTSE, and 10 and 30 mol % AAPTS. Of the controls synthesized with BTSE, AAPTS, and no CTAC, only the 30 mol % AAPTS blank formed any product. This took place only after titrating the basic mixture to pH 8.0 with HCl. The supramolecular assemblies of CTAC seem to catalyze the formation of the organosilicas by providing nucleation sites for the precursor molecules.

Although the batch tests used to estimate the overall accessibility of the diamine sites were performed with 1-h contact times, additional tests with various contact times were performed to ensure that equilibration had been reached within 1 h and to probe the adsorption kinetics in these materials. The PMO synthesized with 10 mol % AAPTS was selected as the adsorbent, and contact times from 60 s to 24 h were used. Surprisingly, spectroscopic analysis of the filtrates indicate that this material adsorbed the same amount of Cu(II) in the first 60 s as it did in 24 h (and all the times between). This is a clear indication that equilibration takes place in less than 60 s. Because it is likely that the Cu(II) is complexed with four or five trizma molecules in this buffer system, the relatively fast adsorption kinetics attest to the open-pore structures in these ordered mesoporous materials.

## Conclusions

PMOs have been synthesized by the co-condensation of BTSE and AAPTS under basic contions. Supramolecular templates of CTAC were used as structure-directing agents. The amount of AAPTS in the initial synthetic mixture has been varied and its effect on the structural and chemical properties of these porous materials has been characterized. Successful removal of the surfactant templates has been accomplished by extracting with acidified ethanol and verified with nitrogen gas sorption, elemental analysis, and thermogravimetric analysis. X-ray diffraction patterns are typical of materials that contain hexagonally packed arrays of mesopores. No significant changes in the *d* spacings were exhibited by any of these PMOs after the extraction step. This indicates that the porous structure in these PMOs remains intact and that these materials exhibit structural rigidity on the molecular scale. Nitrogen sorption analyses show that all the extracted organosilicas exhibit type IV isotherms. As the amount of AAPTS is increased, a gradual decrease in both the BET surface area from 1250 to 910 $m^2/g$ and the total pore volumes from 0.98 to 0.67 $cm^3/g$. All the surfactant-templated PMOs exhibit a sharp peak in their Barrett-Joyner-Halenda (BJH) pore size distributions ~26 Å. The surfactant templated control blank exhibits more than twice the surface area and nearly three times the total pore volume of a nontemplated control sample. Elemental analyses of the organosilica materials indicate that only about one-third of the AAPTS in the original reaction mixture is actually incorporated in the

---

(30) Smith, R. M.; Martell, A. E. *Critical Stability Constants*; Plenum: New York 1975; Vol. 2.

final products. Adsorption of Cu(II)/trizma complexes from aqueous solutions indicate that more than 70% of these functional ligands are accessible for further reaction. Equilibration times for these adsorption processes are less than 60 s.

Future research with these functionalized PMOs will include the optimization of experimental parameters such as pH and reaction time to achieve more efficient incorporation of the AAPTS. The fast access of molecular species to functional groups located within these mesostructures make these organosilicas promising materials for the development of heterogeneous catalysts for both solution and gas-phase reactions.

**Acknowledgment.** M.C.B. is a NRC postdoctoral research fellow. This project was funded by the Office of Naval Research through a Naval Research Laboratory Accelerated Research Initative.

**Supporting Information Available:** X-ray diffraction and nitrogen gas adsorption/desorption isotherms of samples synthesized in this study have been determined (PDF). This material is available free of charge via the Internet at http://pubs.acs.org.

CM0105763